

## 4. PRODUCTION AND PROPERTIES OF RADIATIONS

energy scale measures the distance from the *K*-shell edge energy of germanium (11.104 keV). These curves are taken from Hubbell, McMaster, Del Grande & Mallett (1974). Not only does the experimental curve depart significantly from the theoretically predicted curve, but there is a marked difference in the complexity of the curves between the various germanium compounds.

Far from the absorption edge, the theoretical calculations and the experimental data are in reasonable agreement with what one might expect using the sum rule for the various scattering cross sections and one could say that this region is one in which normal attenuation coefficients may be found.

Closer to the edge, the almost periodic variation of the mass attenuation coefficient is called the extended X-ray absorption fine structure (XAFS). Very close to the edge, more complicated fluctuations occur. These are referred to as X-ray absorption near edge fine structure (XANES). The boundary of the XAFS and XANES regions is somewhat arbitrary, and the physical basis for making the distinction between the two will be outlined in Subsection 4.2.3.4.

Even in the region where normal attenuation may be thought to occur, cooperative effects can exist, which can affect both the Rayleigh and the Compton scattering contributions to the total attenuation cross section. The effect of cooperative Rayleigh scattering has been discussed by Gerward, Thuesen, Stibius-Jensen & Alstrup (1979), Gerward (1981, 1982, 1983), Creagh & Hubbell (1987), and Creagh (1987*a*). That the Compton scattering contribution depends on the physical state of the scattering medium has been discussed by Cooper (1985).

Care must therefore be taken to consider the physical state of the system under investigation when estimates of the theoretical interaction cross sections are made.

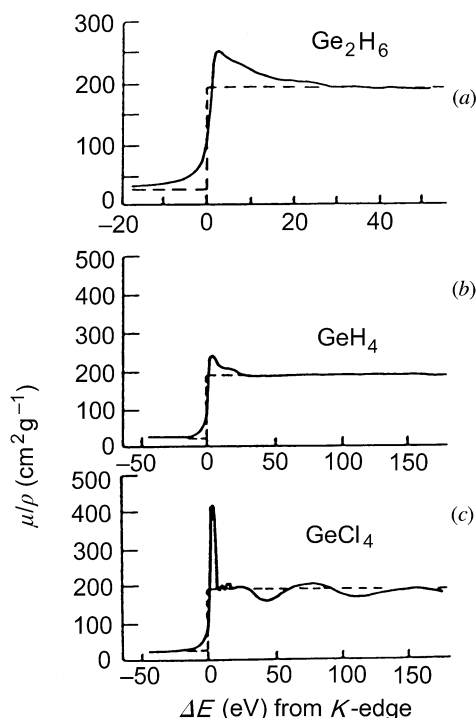


Fig. 4.2.3.2. The dependence of the X-ray attenuation coefficient on energy for a range of germanium compounds, taken in the neighbourhood of the germanium absorption edge (from *IT IV*, 1974).

## 4.2.3.2. Techniques for the measurement of X-ray attenuation coefficients

## 4.2.3.2.1. Experimental configurations

Experimental configurations that set out to determine the X-ray linear attenuation coefficient  $\mu_l$  or the corresponding mass absorption coefficients ( $\mu/\rho$ ) must have characteristics that reflect the underlying assumptions from which equation (4.2.3.1) was derived, namely:

- (i) the incident and transmitted beams are parallel and there is no divergence in the transmitted beam;
- (ii) the photons in the incident and transmitted beams have the same energy;
- (iii) the specimen is of sufficient thickness.

Because of the considerable discrepancies that often exist in X-ray attenuation measurements (see, for example, *IT IV*, 1974), the IUCr Commission on Crystallographic Apparatus set up a project to determine which, if any, of the many techniques for the measurement of X-ray attenuation coefficients is most likely to yield correct results. In the project, a number of different experimental configurations were used. These are shown in Fig. 4.2.3.3. The configurations used ranged in complexity from that

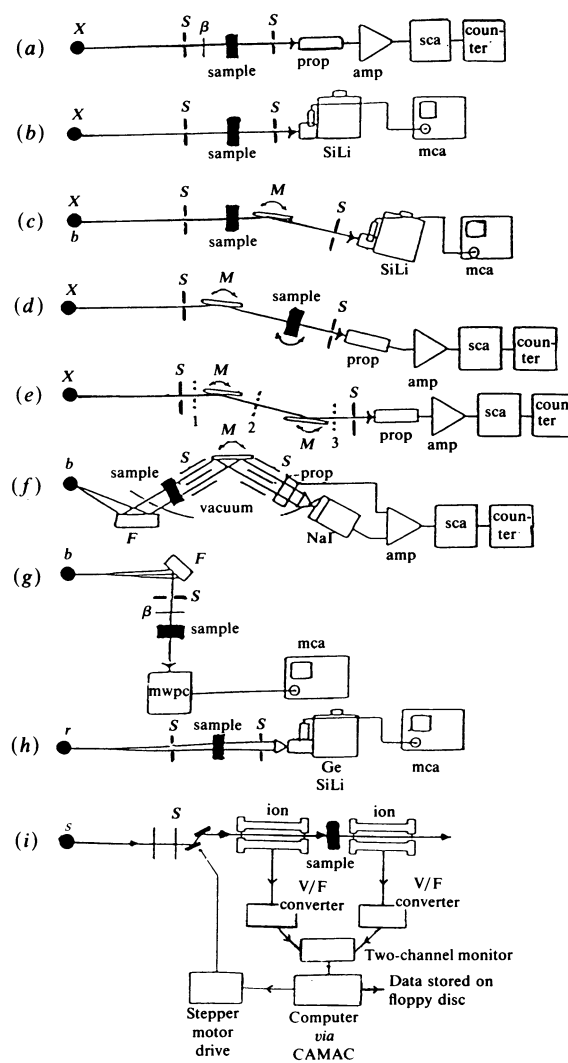


Fig. 4.2.3.3. Schematic representations of experimental apparatus used in the IUCr X-ray Attenuation Project (Creagh & Hubbell, 1987; Creagh, 1985). *X*: characteristic line from sealed X-ray tube; *b*: Bremsstrahlung from a sealed X-ray tube; *r*: radioactive source; *s*: synchrotron-radiation source;  $\beta$ :  $\beta$ -filter for characteristic X-rays; *S*: collimating slits; *M*: monochromator.

## 4.2. X-RAYS

of Fig. 4.2.3.3(a), which uses a slit-collimated beam from a sealed tube and a  $\beta$ -filter to select its characteristic radiation, and a proportional counter and associated electronics to detect the transmitted-beam intensity, to that of Fig. 4.2.3.3(f), which uses a modification to a commercial X-ray-fluorescence analyser. Sources of X-rays included conventional sealed X-ray tubes, X-ray-fluorescence sources, radioisotope sources, and synchrotron-radiation sources. Detectors ranged from simple ionization chambers, which have no capacity for photon energy detection, to solid-state detectors, which provide a relatively high degree of energy discrimination. In a number of cases (Figs. 4.2.3.3c, d, e, and f), monochromatization of the beam was effected using single Bragg reflection from silicon single crystals. In Fig. 4.2.3.3(i), the incident-beam monochromator is using reflections from two Bragg reflectors tuned so as to eliminate harmonic radiation from the source.

The performance of these systems was evaluated for a range of materials that included:

- (i) highly perfect silicon single crystals (Creagh & Hubbell, 1987);
- (ii) polycrystalline copper foils that exhibited a high degree of preferred orientation; and
- (iii) pyrolytic graphite that contained a high density of regular voids.

The results of this study are outlined in Section 4.2.3.2.3.

### 4.2.3.2.2. Specimen selection

Although the most important component in the experiment is the specimen itself, examination of the data files held at the US National Institute of Standards and Technology (Gerstenberg & Hubbell, 1982; Saloman & Hubbell, 1986; Hubbell, Gerstenberg & Saloman, 1986) has shown that, in general, insufficient care has been taken in the past to select an experimental device with characteristics that are appropriate to the specimen chosen. Nor has sufficient care been taken in the determination of the dimensions, homogeneity, and defect structure of the specimens. To achieve the best results, the following procedures should be followed.

(i) The *dimensions* of the specimen should be determined using at least two different techniques, and sample *thicknesses* should be chosen such that the Nordfors (1960) criterion, later confirmed by Sears (1983), that the condition

$$2 \leq \ln(I_0/I) \leq 4 \quad (4.2.3.7)$$

be satisfied. This enables the best compromise between achieving good counting statistics and avoiding multiple photon scattering within the sample.

Wherever possible, different sample thicknesses should be chosen to enable a test of equation (4.2.3.1) to be made. If deviations from equation (4.2.3.1) exist, either the sample material or the experimental configuration, or both, are not appropriate for the measurement of  $\mu_l$ . If the attenuation of the material under test falls outside the limits set by the Nordfors criterion and the material is in the form of a powder, the mixing of this powder with one with low attenuation and no absorption edge in the region of interest can be used to bring the total attenuation of the sample within the Nordfors range.

(ii) The sample should be examined by as many means as possible to ascertain its regularity, homogeneity, defect structure, and, especially for very thin specimens, freedom from pinholes and cracks. Where a diluent has been used to reduce the attenuation so that the Nordfors criterion is satisfied, care must be taken to ensure intimate mixing of the two materials and the absence of voids.

Since the theory upon which equation (4.2.3.1) is based envisages that each atom scatters as an individual, it is necessary to be aware of whether such cooperative effects as Laue–Bragg scattering (which may become significant in single-crystal specimens) and small-angle X-ray scattering (SAXS) (which may occur if a distribution of small voids or inclusions exists) occur in polycrystalline and amorphous specimens. Knowledge that cooperative scattering may occur influences the choice of collimation of the beam.

(iii) The sample should be mounted *normal* to the beam.

### 4.2.3.2.3. Requirements for the absolute measurement of $\mu_l$ or $(\mu/\rho)$

The following prescription should be followed if accurate, absolute measurements of  $\mu_l$  and  $(\mu/\rho)$  are to be obtained.

(i) *X-ray source and X-ray monochromatization.* The *energy* of the incident photons should be measured directly using reflections from a single-crystal silicon monochromator, and the *energy spread* of the beam should be measured. Measurements should be made of the state of *polarization*, since X-ray-polarization effects are known to be significant in some measurements (Templeton & Templeton, 1982, 1985, 1986). The results of a survey on X-ray polarization were given by Jennings (1984). If a single-crystal monochromator is employed, it should be placed between the sample and the detector.

(ii) *Collimation.* It is of some advantage if both the incident-beam- and the transmitted-beam-defining slits can be varied in width.

Should it be necessary to combat the effects of Laue–Bragg scattering in a single-crystal specimen, an incident beam with a high degree of collimation is required (Gerward, 1981).

To counter the effects of small-angle X-ray scattering, it may be necessary to widen the detector aperture (Chipman, 1969). That these effects can be marked has been shown by Parratt, Porteus, Schnopper & Watanabe (1959), who investigated the influence collimator and monochromator configurations have on X-ray-attenuation measurements.

(iii) *Detection.* Detectors that give some degree of energy discrimination should be used. Compromise may be necessary between sensitivity and energy resolution, however, and these factors should be taken into account when a choice is being made between proportional and solid-state detectors.

Whichever detection system is chosen, it is essential that the system dead-time be determined experimentally. For descriptions of techniques for the determination of system dead-time, see, for example, Bertin (1975).

### 4.2.3.3. Normal attenuation coefficients

Fig. 4.2.3.1 shows that the X-ray attenuation coefficients are a smooth function of photon energy over a relatively large range of photon energies, and that discontinuities occur whenever the photon energy corresponds to a resonance in the electron cloud surrounding the nucleus. In Fig. 4.2.3.2, the effect of the interaction of the ejected photoelectron with the electron's neighbouring atoms is shown. Such edge effects (XAFS) can extend 1000 eV from the edge.

It is conventional, however, to extrapolate the smooth curve to the edge value, and a curve of *normal attenuation coefficients* results. These are taken to be the attenuation coefficients of the individual atoms. Tables of these *normal attenuation coefficients* are given in Section 4.2.4.